Molecular Crystals and Liquid Crystals
Publication details, including instructions for authors and subscription information:
http://www.tandfonline.com/loi/gmcl20

Synthesis and Physical Properties of Ferrocene Derivatives (XXV) Liquid Crystallinity of 1,3-Disubstituted Ferrocene Derivatives

Naotake Nakamura [a] & Shinya Kagawa [a]
[a] Department of Applied Chemistry, College of Life Sciences, Ritsumeikan University, 1-1-1, Nojihigashi, Kusatsu, Shiga 525-8577, Japan

Version of record first published: 07 Oct 2011

To cite this article: Naotake Nakamura & Shinya Kagawa (2011): Synthesis and Physical Properties of Ferrocene Derivatives (XXV) Liquid Crystallinity of 1,3-Disubstituted Ferrocene Derivatives, Molecular Crystals and Liquid Crystals, 549:1, 150-159

To link to this article: http://dx.doi.org/10.1080/15421406.2011.581526

Mol. Cryst. Liq. Cryst., Vol. 549: pp. 150–159, 2011

ISSN: 1542-1406 print/1563-5287 online
DOI: 10.1080/15421406.2011.581526

Synthesis and Physical Properties of Ferrocene Derivatives (XXV) Liquid Crystallinity of 1,3-Disubstituted Ferrocene Derivatives

NAOTAKE NAKAMURA* AND SHINYA KAGAWA

Department of Applied Chemistry, College of Life Sciences, Ritsumeikan University, 1-1-1, Nojihigashi, Kusatsu, Shiga 525-8577, Japan

Liquid crystallinity of 1,3-disubstituted ferrocene derivatives was studied by DSC and polarizing microscope. The name of the derivatives is 1,3-bis[ω-[4-(4-methoxyphenoxycarbonyl)phenoxy]alkyloxycarbonyl]ferrocene. Nine members from n = *2 to 10 were synthesized (*n *is carbon number of alkyl chain in the sample). All samples except* n = *2 and 4 exhibited monotropic nematic liquid crystalline phase. In addition, smectic X (not yet completely identified) was also observed in* n = *8 and 10. Liquid crystalline phase transition phenomena were discussed from a viewpoint of molecular shape.*

1. Introduction

The iron is one of the transitional metals, and ferrocene contains one iron atom in its molecule. If liquid crystals containing ferrocene are synthesized, they are expected to show many interesting physical properties such as electric, magnetic, and so on, in addition to liquid crystallinity. It is possible to introduce not only one substituent including a mesogenic group but also two or three ones into ferrocenyl moiety, because ferrocene molecule has two cyclopentadienyl rings which easily undergo a substituted reaction like benzene. Therefore, widely different kind of ferrocene derivatives, for example, monosubstituted ferrocene derivatives, 1,1′-disubstituted ones and 1,3-disubstituted ones, have been studied by many researchers and many papers have been published up to now [1].

Liquid crystalline monosubstituted ferrocene derivatives were firstly reported by J. Malthéte and J. Billard in 1976 [2], and J. Bhatt and coworkers reported liquid crystalline 1,1′- disubstituted ones in 1988 [3].

R. Deschenaux and J.-L. Marendaz reported 1,3-disubstituted ferrocene-containing liquid crystals, as an initial study in 1991 [4]. They synthesized 1,3-bis[ω-4-(4-n-alkoxyphenylcarbonyloxy)phenoxycarbonyl]ferrocene. Here, the number of carbon atom in alkoxyl terminal group was abbreviated as *cn*. They prepared 16 members, of which *cn* is from 1 to 18, except *cn* = 15 and 17. All members exhibited enantiotropic liquid crystallinity, more specifically, nematic phase was observed in the members from *cn* = 1 to 16. Smectic C phase appeared only above *cn* = 12 in addition to nematic one. Here, the smectic C phase in *cn* = 12 were observed in cooling process only, and *cn* = 18 exhibited

*Corresponding author. E-mail: nakamura@sk.ritsumei.ac.jp

enantiotropic smectic C phase only. The molecular and crystal structure analyses were carried out by X-ray diffraction method, and "T" shaped molecular structure was found out [5].

We have been studied liquid crystallinity of monosubstituted ferrocene derivatives since 1993 [6–8] and 1,1′-disubstituted ones since 1994 [9,10].

Many reports on structural study of the monosubstituted ferrocene derivatives [11–19] and 1,1′-disubstituted ones [20–24] were presented by N.Nakamura and his coworkers. Recently, a new paper on the relationship between liquid crystallinity and the structural data among all the monosubstituted homologues, and a structural comparison between the monosubstituted ferrocene derivatives and the 1,1′-disubstituted ones were made [25].

In this work, 1,3-disubstituted ferrocene derivatives were newly designed, synthesized and investigated on its liquid crystallinity. The structural feature of the samples studied here is that the substituents including mesogenic groups are the same as those of monosubstituted [8] and 1,1′-disubstituted ferrocene derivatives [9,10], previously studied in our laboratory.

2. Experimental

Nine members of 1,3-bis[ω-[4-(4′-methoxyphenoxycarbonyl)phenoxy]alkyloxycarbonyl]-ferrocene (abbreviated here after 1,3-bMAF-*n*, *n* is carbon number of alkyl chain in the sample. n = 2-10) have been synthesized. General chemical structure of 1,3-bMAF-*n* is shown in Figure 1. A flexible alkyl chain exists between the mesogenic group and the ferrocenyl moiety. It is considered that the flexible alkyl chain plays an important role to compensate the bulky effect of the ferrocenyl moiety, because the existence of the ferrocenyl moiety may hinder to make a linear molecular shape, which is rod-like one. As is well known, the linear molecular shape is desirable to show liquid crystallinity. The synthetic route is shown in Figure 2. Purifications of all intermediate products and objective compounds were repeated many times and judged to be pure by TLC which showed only one spot. The compounds obtained here are identified as objective compounds using ^{1}H-NMR(JEOL ECS-400).

As an example, the reaction condition and yield of 1,3-bMAF-5 are described below, because 1,3-bMAF-5 is one of the liquid crystalline derivatives of 1,3-bMAF-*n*.

1) Starting material, commercially available acetylferrocene, was reduced by $LiAlH_4$ with $AlCl_3$ under room temperature. Ethylferrocene was obtained. Yield was 82.0%.
2) Ethylferrocene was converted to 1-acetyl-3-ethylferrocene using acetic anhydride under room temperature. Reaction mixture was treated by open column chromatography for separation and purification. Yield was 88.1%.
3) Ethyl group of 1-acetyl-3-ethylferrocene was oxidized to acetyl group by MnO_2 under 60°C, and obtained 1,3-diacetylferrocene. Yield is 1.9%.
4) 1,3-ferrocenyl dicarboxylic acid was obtained from 1,3-diacetylferrocene using NaOBr after stirring 1 hr on ice bath and 3 hr stirring under room temperature. Yield was 72.0%.

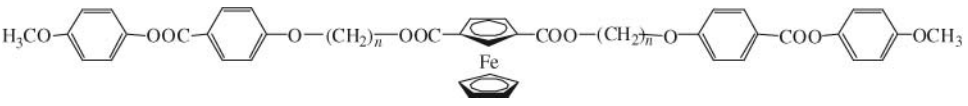

Figure 1. General chemical structure of 1,3-bMAF-*n*.

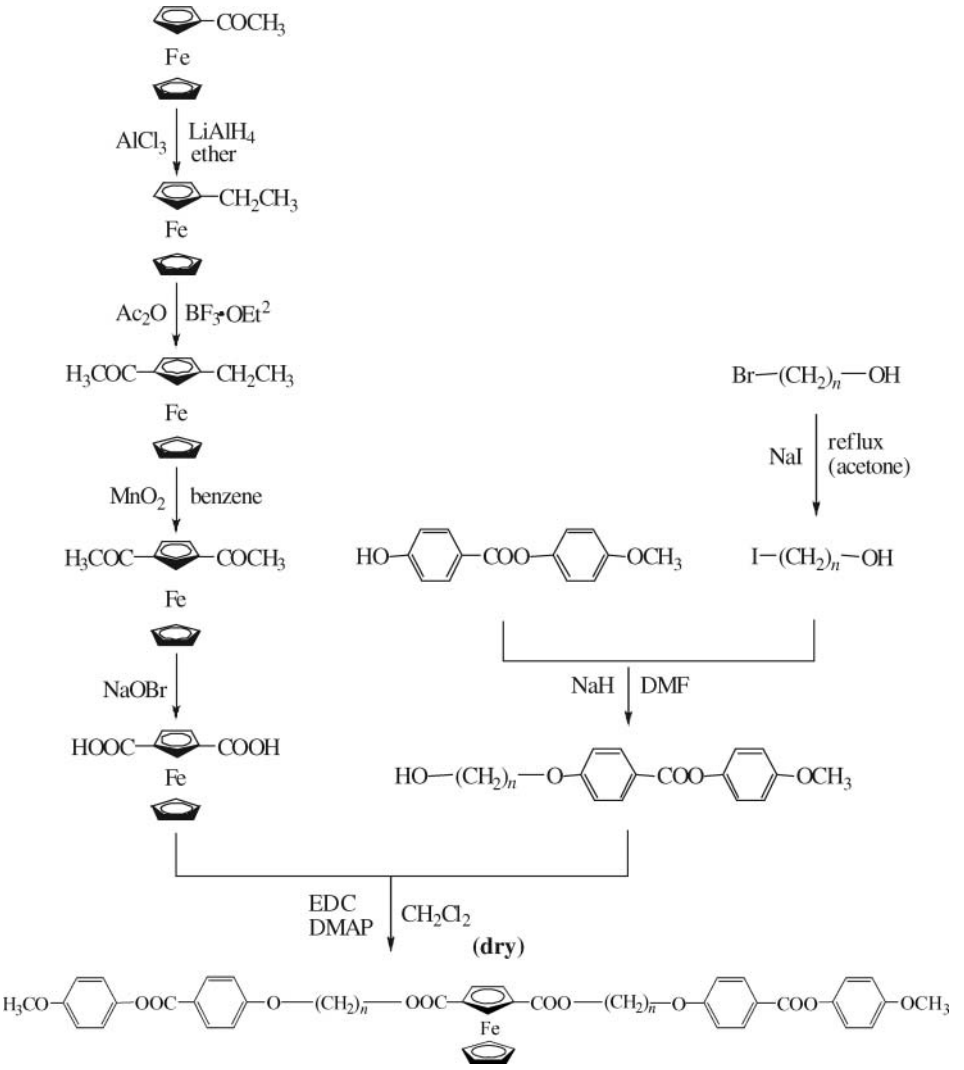

Figure 2. Synthetic route of 1,3-bMAF-*n*.

5) Halogen exchange reaction from Br to I was carried out. That is, commercially available 5-bromopentane-1-ol was refluxed 3hr with NaI under 65°C, and 5-iodopentane-1-ol was obtained. Yield was 88.9%.
6) 4′-Methoxyphenyl-4-hydroxybenzoate was etherified with 5-iodopentane-1-ol by stirring 24hr under 50°C. Reaction mixture was treated by open column chromatography. Yield was 41.5%.
7) 1,3-Ferrocenyl dicarboxylic acid was esterified with the compound obtained above by stirring 24 hr under room temperature, in order to obtain objective compound. Reaction mixture was treated by open column chromatography. Yield was 63.0%.

In Figure 3, ^{1}H-NMR spectrum of 1,3-bMAF-5 is shown, as an example. All protons were marked by A-J and α-γ, as mentioned in upper part of Figure 3. Corresponding peaks

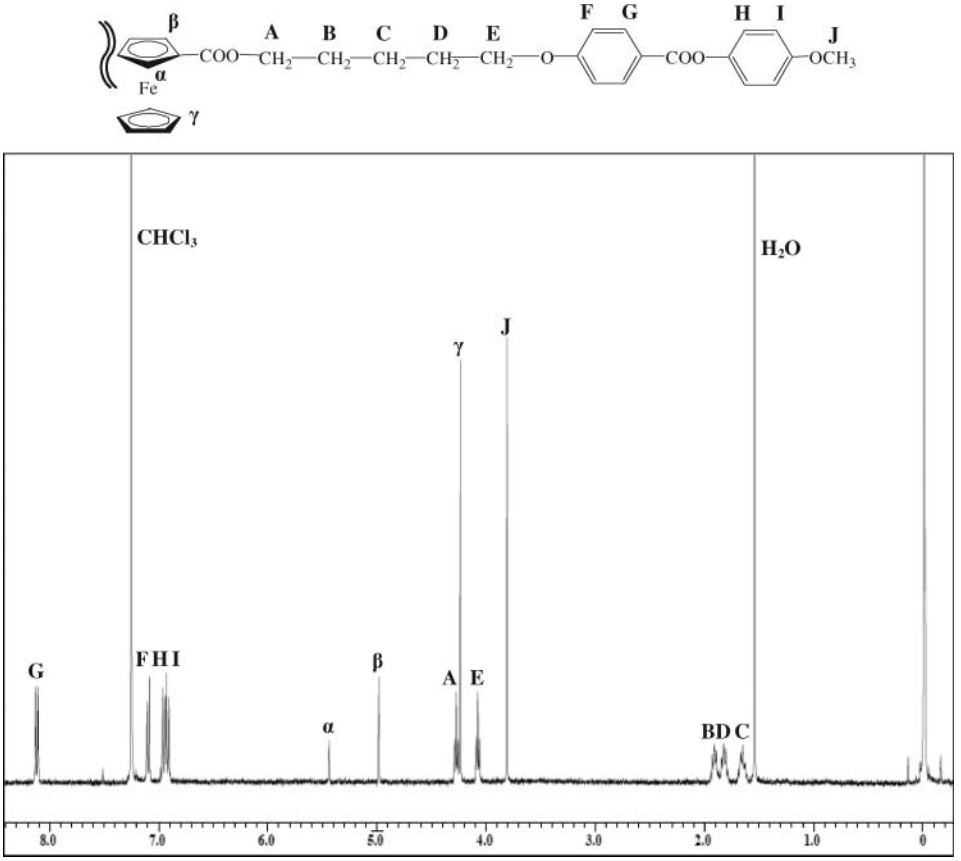

Figure 3. ^{1}H-NMR spectrum of 1,3-bMAF-**5**.

in Figure 3 were also marked by A-J and α-γ. The identification was carried out by this way for all samples.

Obtained ^{1}H-NMR δ-values of all samples studied here are mentioned below.

1,3-bMAF-2

δ 8.15(*d*, 4H, $J = 8.68$), 7.09(*d*, 4H, $J = 9.16$), 7.01(*d*, 4H, $J = 8.72$), 6.91(*d*, 4H, $J = 9.16$), 5.48(*s*, 1H,), 5.02(*d*, 2H, $J = 0.92$), 4.62(*t*, 4H, $J = 3.87$), 4.36(*t*, 4H, $J = 4.58$), 4.20(*s*, 5H), 3.81(*s*, 6H,)

1,3-bMAF-3

δ 8.13(*d*, 4H, $J = 9.16$), 7.09(*d*, 4H, $J = 9.16$), 6.98(*d*, 4H, $J = 8.48$), 6.91(*d*, 4H, $J = 9.16$), 5.42(*s*, 1H), 4.98(*d*, 2H, $J = 1.36$), 4.44(*t*, 4H, $J = 6.40$), 4.21(*t*, 4H, $J = 5.96$), 4.16(s, 5H), 3.80(*s*, 6H), 2.25(*d*, 4H, $J = 6.29$),

1,3-bMAF-4

δ 8.12(*d*, 4H, $J = 8.68$), 7.10(*d*, 4H, $J = 9.16$), 6.96(*d*, 4H, $J = 8.68$), 6.91(*d*, 4H, $J = 9.16$), 5.43(*s*, 1H), 4.98(*d*, 2H, $J = 0.92$), 4.32(t, 4H, $J = 5.96$), 4.24(*s*, 5H), 4.12(*t*, 4H, $J = 5.72$), 3.80(*s*, 6H), 1.96(*br,* 8H,)

1,3-bMAF-5

δ 8.12(*d*, 4H, $J = 8.68$), 7.10(*d*, 4H, $J = 9.16$), 6.96(*d*, 4H, $J = 8.68$), 6.91(*d*, 4H, $J = 9.16$), 5.43(*s*, 1H), 4.98(*d*, 2H, $J = 0.92$), 4.32(t, 4H, $J = 5.96$), 4.24(*s*, 5H), 4.12(*t*, 4H,

$J = 5.72$), 3.80(*s*, 6H), 1.86(*quin*, 4H, $J = 6.63$), 1.77(*quin*, 4H, $J = 6.75$), 1.64(*quin*, 4H, $J = 6.75$)

1,3-bMAF-6

δ 8.11(*d*, 4H, $J = 8.68$), 7.09(*d*, 4H, $J = 8.72$), 6.94(*d*, 4H, $J = 8.68$), 6.91(*d*, 4H, $J = 9.16$), 5.42(*s*, 1H), 4.97(*d*, 2H, $J = 0.68$), 4.24(*t*, 4H, $J = 7.56$), 4.22(*s*, 5H), 4.05(*t*, 4H, $J = 6.18$), 3.80(*s*, 6H), 1.86(*quin*, 4H, $J = 6.63$), 1.77(*quin*, 4H, $J = 6.75$), 1.54(*br*, 8H)

1,3-bMAF-7

δ 8.11(*d*, 4H, $J = 8.24$), 7.09(*d*, 4H, $J = 8.72$), 6.94(*m*, 8H), 5.42(*s*, 1H), 4.97(*s*, 2H), 4.22(*t*, 4H, $J = 6.86$) 4.22(*s*, 5H, $J = 6.86$), 4.03(*t*, 4H, $J = 6.40$), 3.81(*s*, 6H), 1.83(*quin*, 4H, $J = 6.87$), 1.74(*quin*, 4H, $J = 6.98$), 1.47(*br*, 12H)

1,3-bMAF-8

δ 8.11(*d*, 4H, $J = 9.16$), 7.09(*d*, 4H, $J = 9.16$), 6.92(*m*, 8H), 5.42(*s*, 1H) 4.97(*d*, 2H, $J = 1.40$), 4.22(*t*, 4H, $J = 7.56$), 4.22(*s*, 5H, $J = 7.56$) 4.02(*t*, 4H, $J = 7.93$), 3.80(*s*, 6H), 1.82(*quin*, 4H, $J = 7.10$), 1.73(*quin*, 4H, $J = 6.87$), 1.41(*br*, 16H)

1,3-bMAF-9

δ 8.11(*d*, 4H, $J = 9.16$), 7.09(*d*, 4H, $J = 9.16$), 6.92(*m*, 8H), 5.42(*s*, 1H), 4.96(*d*, 2H, $J = 1.36$), 4.22(*t*, 4H, $J = 4.41$), 4.22(*s*, 5H, $J = 4.41$),4.01(*t*, 4H, $J = 6.64$), 3.80(*s*, 6H), 1.80(*quin*, 4H, $J = 6.98$), 1.72(*quin*, 4H, $J = 6.87$), 1.37(*br*, 20H)

1,3-bMAF-10

δ 8.11(*d*, 4H, $J = 9.16$), 7.09(*d*, 4H, $J = 9.16$), 6.92(*m*, 8H), 5.42(*s*, 1H), 4.96(*d*, 2H, $J = 1.36$), 4.22(*t*, 4H, $J = 4.41$), 4.22(*s*, 5H, $J = 4.41$),4.01(*t*, 4H, $J = 6.64$), 3.80(*s*, 6H), 1.80(*quin*, 4H, $J = 6.98$), 1.72(*quin*, 4H, $J = 6.87$), 1.32(*br*, 24H)

Phase transition phenomena were studied by polarizing microscope (Nikon XTP-11) equipped with temperature controller system (Mettler FP800 and Mettler FP82HT Hot Stage), and DSC (Perkin Elmer Pyris 1) of which temperature and calorie are calibrated using 99.9999% indium. Scanning rate of these apparatuses is 5°C/min.

3. Results and Discussion

As an example, DSC chart of 1,3-bMAF-2 is shown in Figure 4. On the first heating process, peak A corresponding to melting point of unstable solid crystal was observed, and recrystallization underwent continuously showing peak B. Peak C was the melting point

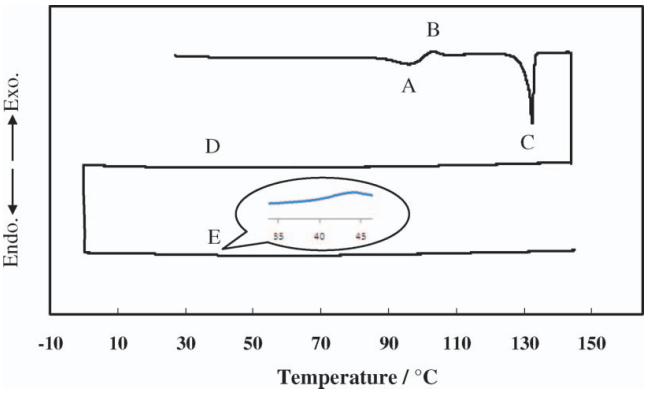

Figure 4. DSC chart of 1,3-bMAF-2 (5.0°C/min).

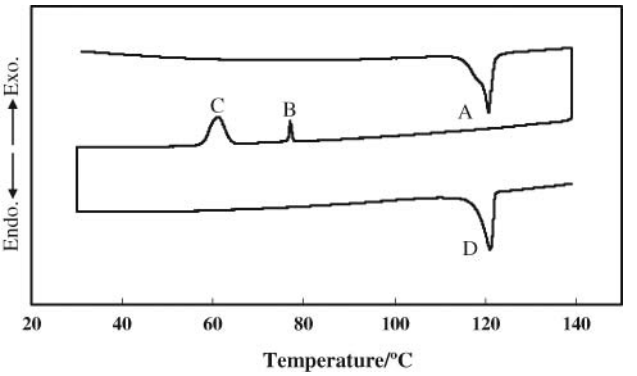

Figure 5. DSC chart of 1,3-bMAF-5 (5.0°C/min).

of stable solid. On the first cooling and second heating processes, glass transition points were observed at D and E. As it is difficult to see the glass transition points in this Figure, enlarged glass transition point E was illustrated in the Figure. That is, no liquid crystalline phase transition points observed on the cooling and the heating processes. As an another example, DSC chart and texture of 1,3-bMAF-5 are shown in Figures 5 and 6, respectively. On the first heating process, peak A was observed at 121°C as melting point, where the temperature was measured by onset one. Peaks B and C were observed at 77 and 61 °C on the first cooling process as phase transition point from isotropic liquid to liquid crystalline phase and that from the liquid crystalline phase to solid crystal, respectively. This phase observed above was identified as liquid crystalline nematic phase from the typical texture shown in Figure 6, because its Schlieren texture strongly suggested nematic phase. On the second heating process, only one peak D was observed. This point was judged to be the melting point from the polarizing microscopic observation.

Phase transition phenomena observed here were summarized in Figure 7. Allmembers except 1,3-bMAF-2 and 4 showed monotropic liquid crystalline phase. A few hystereses of the transition points were observed. The phenomena were sometimes seen on monotropic phase transition. In addition, phase transition temperatures measured by DSC were depending on the scanning rate. These liquid crystalline phases were identified as nematic phase by the texture observation using the polarizing microscope as mentioned above. Another liquid crystalline phase was observed at lower temperature side in 1,3-bMAF-8 and 10. This lower temperature phase was identified as smectic one from the typical texture observed by the polarizing microscope. As is well known, widely different kind of smectic phases have been authorized. As this smectic phase is not yet completely identified in this work, the phase observed here is named as SmX in Figure 7, temporarily.

Figure 8 exhibits the relation between carbon number of alkyl chain (n) and the transition temperature from isotropic liquid to liquid crystalline phase observed on the first cooling process.

Even-odd effect is clearly observed in Figure 8. This effect is considered as follows.

Molecular models of 1,3-bMAF-3 and 4 designed by Chem 3D Ultra program as examples of odd member and even one are presented in Figures 9 and 10, respectively. Simplified molecular models are also shown in Figures 11 and 12, respectively. It is easily understood that 1,3-bMAF-3 is rod like while 1,3-bMAF-4 is curved. Namely, molecular shape of the odd members is regarded as the rod like, which is desirable to appear liquid crystalline phase. It becomes more desirable with increasing carbon number in the alkyl chain, because

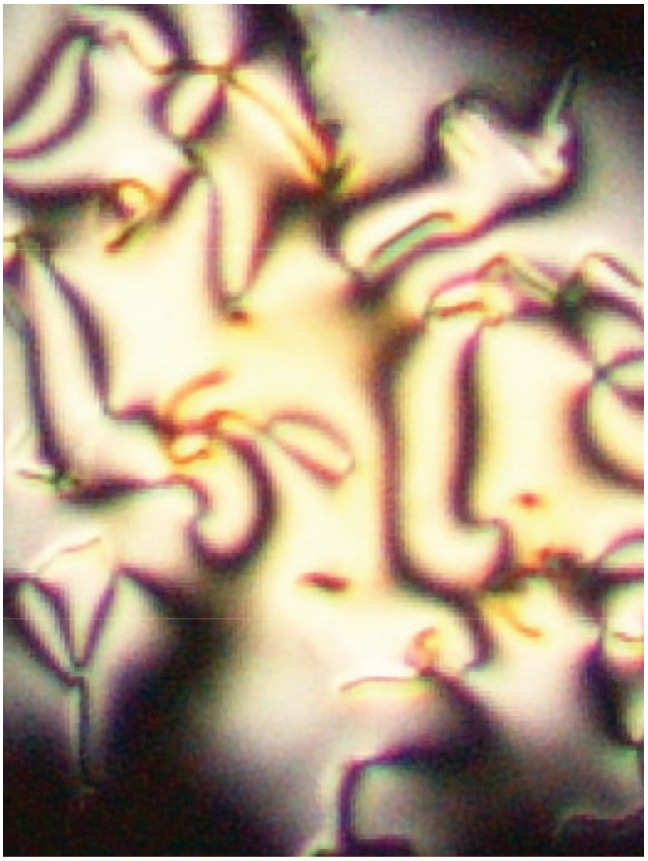

Figure 6. Optical texture of 1,3-bMAF-5 taken at 74°C under the polarizing microscope (×400).

n	Phase transition temperature / °C
2	G $\underset{39}{\overset{39}{\rightleftharpoons}}$ I.L.
3	K1 $\underset{63}{\overset{132}{\rightleftharpoons}}$ N $\underset{66}{\overset{148}{\rightleftharpoons}}$ I.L
4	G $\underset{23}{\overset{23}{\rightleftharpoons}}$ I.L.
5	K1 $\underset{61}{\overset{121}{\rightleftharpoons}}$ N $\underset{77}{\overset{}{\rightleftharpoons}}$ I.L.
6	G $\underset{8}{\overset{8}{\rightleftharpoons}}$ N $\underset{45}{\overset{46}{\rightleftharpoons}}$ I.L.
7	K1 $\underset{69}{\overset{123}{\rightleftharpoons}}$ N $\underset{76}{\overset{}{\rightleftharpoons}}$ I.L.
8	SmX $\underset{42}{\overset{35}{\rightleftharpoons}}$ K1 $\underset{N}{\overset{99}{\rightleftharpoons}}$ K2 $\underset{56}{\overset{117}{\rightleftharpoons}}$ I.L.
9	K1 $\underset{69}{\overset{121}{\rightleftharpoons}}$ N $\underset{71}{\overset{}{\rightleftharpoons}}$ I.L.
10	SmX $\underset{53}{\overset{17}{\rightleftharpoons}}$ K1 $\underset{N}{\overset{118}{\rightleftharpoons}}$ I.L.

G : glass state
I.L : isotropic liquid state
N : nematic phase
SmX : unidentified smectic phase
K1, K2: crystalline phase

Figure 7. Phase transition temperature of liquid crystalline 1,3-bMAF-*n*.

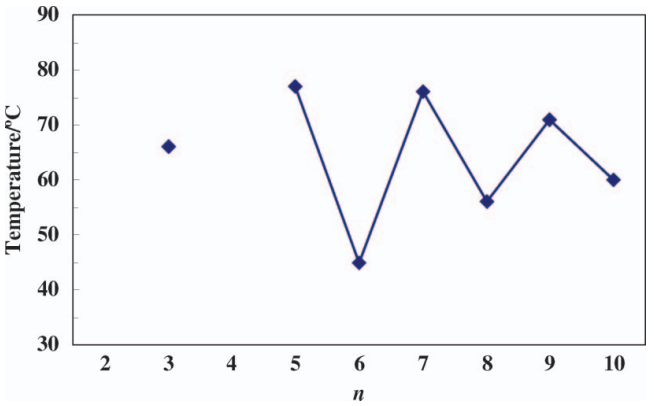

Figure 8. Transition temperature of 1,3-bMAF-*n* on cooling process against the carbon number of alkyl chain (*n*).

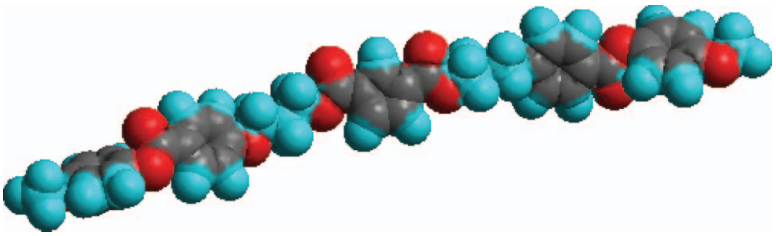

Figure 9. Molecular structure of 1,3-bMAF-3 drawn by Chem 3D Ultra.

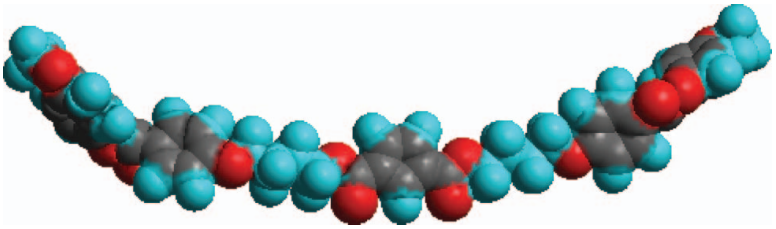

Figure 10. Molecular structure of 1,3-bMAF-4 drawn by Chem 3D Ultra.

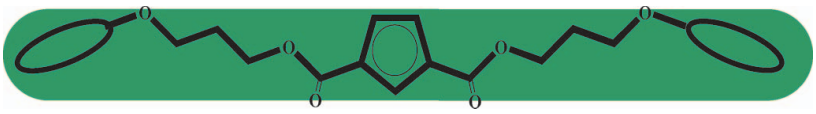

Figure 11. Simplified molecular models for the odd members.

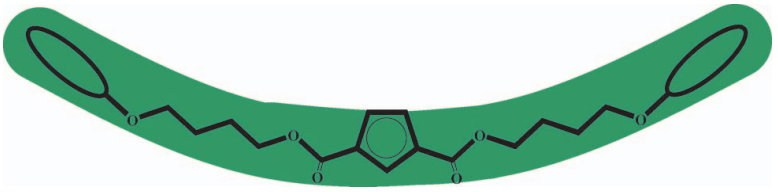

Figure 12. Simplified molecular models for the even members.

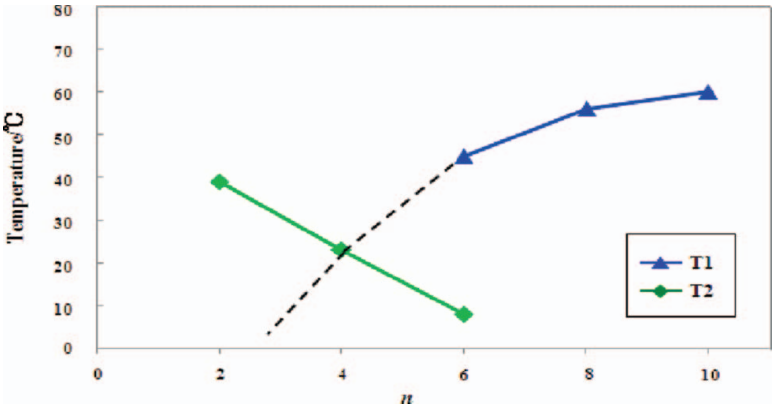

Figure 13. Transition temperature of 1,3-bMAF-*n* against the carbon number of alkyl chain (*n*), (even number).

the aspect ratio increases with increasing alkyl chain length. On the other hand, the transition temperature from isotropic liquid to liquid crystalline phase of even members is rather low compared with that of odd ones. It is considered that the molecular shape of even members is curved a little as is shown in the Figures 10 and 12. The curved effect might be compensated a little with increasing carbon number of the alkyl chain, but this compensational effect is not large enough to turn over the transition temperature of odd members.

Temperature dependence of the transition temperatures of even members is shown in Figure 13. The transition temperature from isotropic liquid to liquid crystalline phase (T1) descends gradually with decreasing carbon number of alkyl chain. On the other hand, glass transition point (T2) also gradually descends with increasing carbon number (*n*). As a result, these two lines cross each other at around $n = 4$. Therefore, T1 of 1,3-bMAF-2 may appear too low from T2. In fact, 1,3-bMAF-2 didn't show the liquid crystalline phase. Similarly, 1,3-bMAF-4 also didn't show the liquid crystalline phase by the same reason. It is considered that this is one of the reason why 1,3-bMAF-2 and 4 show no liquid crystalline phase.

Acknowledgement

A High-Tech Research Center Project for Private Universities matching fund subsidy from MEXT (Ministry of Education, Culture, Sports, Science and Technology), 2006-2010 is gratefully acknowledged for partial financial support of the present work.

References

[1] D.W. Bruce, R. Deschenaux, B. Donnio, and D. Guillon, *Comprehensive Organometallic Chemistry III* **12**, 195–293 (2007). Eds: R. Crabtree and M. Mingos, Elsevier Science, GRB.
[2] J. Malthéte and J. Billard, *Mol. Cyst. Liq. Cryst.* **34**, 177–121 (1976).
[3] J. Bhatt, B.M. Fung, K.M. Nicholas, and C.-D. Poon, *J. Chem. Soc. Chem. Commun.* **1988**, 1439–1439 (1988).
[4] R. Deschenaux and J-L. Marendaz, *J. Chem. Soc., Chem. Commun.* **1991**, 909–910.
[5] R. Deschenaux, I. Kosztics, J-L. Marendaz, and H. Stoeckli-Evans, *Chimia* **47**, 206–210 (1993).
[6] N. Nakamura, T. Hanasaki, and H. Onoi, *Mol. Cyst. Liq. Cryst.* **225**, 269–277 (1993).
[7] T. Hanasaki, M. Ueda, and N. Nakamura, *Mol. Cyst. Liq. Cryst.* **237**, 329–336 (1993).
[8] N. Nakamura, K. Hiro, M. Nishikawa, T. Okabe, and K. Uno, *Mol. Cyst. Liq. Cryst.* **516**, 122–131 (2010).
[9] T. Hanasaki, M. Ueda, and N. Nakamura, *Mol. Cyst. Liq. Cryst.* **250**, 257–267 (1994).
[10] N. Nakamura, R. Mizoguchi, M. Ueda, and T. Hanasaki, *Mol. Cyst. Liq. Cryst.* **312**, 127–136 (1998).
[11] N. Nakamura and S. Setodoi, *Mol. Cyst. Liq. Cryst.* **319**, 173–181 (1998).
[12] N. Nakamura and S. Setodoi, *Mol. Cyst. Liq. Cryst.* **312**, 253–261 (1998).
[13] N. Nakamura and S. Setodoi, *Mol. Cyst. Liq. Cryst.* **326**, 177–187 (1999).
[14] N. Nakamura and S. Setodoi, *Mol. Cyst. Liq. Cryst.* **333**, 151–163 (1999).
[15] N. Nakamura, S. Setodoi, and T. Hanasaki, *Mol. Cyst. Liq. Cryst.* **350**, 93–101 (2000).
[16] N. Nakamura, S. Setodoi, and T. Takayama, *Mol. Cyst. Liq. Cryst.* **346**, 19–28 (2000).
[17] N. Nakamura, T. Takahashi, K. Uno, and T. Hanasaki, *Mol. Cyst. Liq. Cryst.* **383**, 27–35 (2002).
[18] N. Nakamura, T. Nio, and T. Okabe, *Mol. Cyst. Liq. Cryst.* **460**, 85–92 (2006).
[19] N. Nakamura, T. Nio, and T. Okabe, *Mol. Cyst. Liq. Cryst.* **461**, 29–36 (2007).
[20] N. Nakamura and T. Okabe, *Chem. Lett.* **33**, 358–359 (2004).
[21] N. Nakamura and M. Nishikawa, *Chem. Lett.* **34**, 1544–1545 (2005).
[22] N. Nakamura, T. Okabe, and T. Takahashi, *Mol. Cyst. Liq. Cryst.* **441**, 243–250 (2005).
[23] N. Nakamura, T. Nio, T. Okabe, B. Donnio, D. Guillon, and J.-L. Gallani, *Mol. Cyst. Liq. Cryst.* **466**, 3–12 (2007).
[24] T. Okabe, K. Nakazaki, T. Igaue, N. Nakamura, B. Donnio, D. Guillon, and J-L. Gallani, *J. Appl. Cryst.* **42**, 63–68 (2009).
[25] N. Nakamura, K. Hiro, and K. Uno, *Proc. of SPIE* **7775**, 77750O1–77750O7 (2010).